JOURNAL OF Materials CHEMISTRY

Photoluminescent multilayer films based on polyoxometalates†

Lin Xu,[a] Hongyu Zhang,[a] Enbo Wang,*[a,b] Dirk G. Kurth[c] and Zhuang Li[d]

[a]*Department of Chemistry, Northeast Normal University, Changchun 130024, P. R. China. E-mail: linxu@nenu.edu.cn; Fax: +86 431 5684009*
[b]*Coordination Chemistry Institute, State Key Laboratory of Nanjing University, Nanjing 210093, P. R. China*
[c]*Max-Planck-Institute of Colloids and Interfaces, D-14424 Potsdam, Germany*
[d]*Changchun Institute of Applied Chemistry, Academia Sinica, Changchun 130022, P. R. China*

Received 12th September 2001, Accepted 13th November 2001
First published as an Advance Article on the web 28th January 2002

Ultrathin multilayer films consisting of the polyoxotungstoeuropate cluster $K_{12}[EuP_5W_{30}O_{110}]$ (EuP_5W_{30}) and poly(allylamine hydrochloride) (PAH) have been prepared by the layer-by-layer self-assembly method. The (EuP_5W_{30}/PAH) multilayer films have been characterized by small-angle X-ray reflectivity measurements, X-ray photoelectron spectra, and atomic force microscopy (AFM). From the AFM images, the thickness of the {PEI/PSS/PAH(EuW_{30}/PAH)} multilayer film was estimated to be 6.5 nm, corresponding to an average thickness of *ca.*1.1 nm for a EuW_{30}/PAH layer pair. The photoluminescent behavior of the film at room temperature was investigated to show the characteristic Eu^{3+} emission pattern of $^5D_0 \rightarrow {}^7F_J$. The fluorescence behavior of the multilayer film is essentially identical to that of $H_n[EuP_5W_{30}O_{110}]^{(12-n)-}$ in a concentrated aqueous solution, except for the relative intensities and peak bandwidths. The occurence of photoluminescent activity confirms the potential for creating luminescent multilayers with polyoxometalates (see ref. 23).

Introduction

Over the past few years, the fabrication of self-assembled ultrathin films has attracted considerable interest because of their importance in the design of nanostructured materials with tailored structures and properties.[1] The layer-by-layer (LbL) self-assembly method, initially developed for pairs of oppositely charged polyelectrolytes,[2] is a facile and versatile technique that has recently emerged as a viable approach to the preparation of large area ultrathin films. Many different multilayers with nanocrystallites, colloidal gold, titanium dioxide, magnetite nanoparticles and other functional components incorporated into polymer matrices have been fabricated.[3–9]

Polyoxometalates (POMs), a class of molecularly defined inorganic metal oxide clusters, possess intriguing structures and diverse properties and, therefore, are attracting increasing attention worldwide.[10,11] The relevant properties related to developing functional materials are (i) catalytic activity for chemical transformations,[12] (ii) molecule-based conductivity,[13] (iii) magnetism,[14] as well as (iv) photochromism, electrochromism, and luminescence.[15] Obviously, polyoxometalates are extremely versatile inorganic building blocks for the construction of functional materials. However, their potential application in electrocatalysis, molecular electronics, and electro-optical devices requires successful fabrication of thin films.[16] Ichinose *et al.* prepared multilayer films of isopolymolybdate ($(NH_4)_4[Mo_8O_{26}]$) by means of alternate adsorption of POM and poly(allylamine hydrochloride) (PAH).[17] Kurth's group recently reported the preparation of two ultrathin multilayer polyoxometalate–polyelectrolyte films, incorporating the polyoxometalate cluster $(NH_4)_{21}[H_3Mo_{57}V_6(NO)_6O_{183}(H_2O)_{18}]$ as well as the Keplerate cluster $(NH_4)_{42}[Mo_{132}O_{372}(CH_3COO)_{30}(H_2O)_{72}]$, by the LbL method.[18,19] Their results demonstrate that the LbL method is also applicable for the fabrication of multilayer films of anionic POMs and polycationic PAH. However, to our knowledge, the exploration of POM-based multilayer films as functional materials is relatively rare.[20,21] For this, it will be of critical importance to successfully incorporate the functional properties of POMs into the ultrathin material. In this paper, we describe a photoluminescent POM-based LbL multilayer film prepared from both polyoxotungstoeuropate $K_{12}[EuP_5W_{30}O_{110}]$ (EuP_5W_{30}) and positively charged polyelectrolytes.

Experimental

Materials

Polyoxotungstoeuropate, $K_{12}[EuP_5W_{30}O_{110}]\cdot 54H_2O$, was prepared according to the literature method,[22] and the product was recrystallized twice. IR (KBr): 1161.94, 1091.65, 959.18, 911.54, 780.68 cm^{-1}. Poly(ethyleneimine) (PEI; MW 50,000), poly(styrenesulfonate) (PSS; MW 70,000), and poly(allylamine hydrochloride) (PAH; MW 70,000) were purchased from Aldrich and were used without further treatment. The water used in all experiments was deionized to a resistivity of 17–18 MΩ cm.

Characterization of the films

UV-vis absorption spectra were recorded on a quartz slide using a 756CRT UV-visible spectrophotometer. X-Ray photoelectron spectroscopy (XPS) was carried out on a silicon wafer using an Escalab-MK II photoelectronic spectrometer with ALK2(1486.6 eV) as the excitation source. X-Ray reflectivity (XRR) experiments were performed with a Philips X'Pert instrument using Cu-Kα radiation ($\lambda = 1.5405$ Å). XRR measurements for the multilayer film deposited on a silicon wafer yielded data similar to that on quartz substrates. AFM images were taken on mica slides using a Digital Instruments Nanoscope IIIa instrument operating in the tapping mode with

†XRR spectrum of {(PEI/PSS/PAH)(EuP_5W_{30}/PAH)$_6$}, UV-Vis spectrum of EuP_5W_{30} anion and AFM image of the top layer of (PEI/PSS/PAH). See http://www.rsc.org/suppdata/jm/b1/b108283c/

 DOI: 10.1039/b108283c

silicon nitride tips. Photoluminescence spectra were measured using a SPEX FL-2T2 instrument with a 450 W xenon lamp monochromatized by a double grating (1200 grooves mm^{-1}).

Preparation of the films

The cleaned substrates (quartz, silicon, or mica), were immersed in a 1×10^{-2} mol L^{-1} PEI solution for 20 min, rinsed with water, and dried under a nitrogen stream. The PEI-coated substrates were then exposed to a 1×10^{-2} mol L^{-1} PSS solution for 20 min, followed by alternating 20 min immersions in 1×10^{-2} mol L^{-1} PAH solution (containing 1 mol L^{-1} NaCl; pH $\approx$ 2.5–3) and EuP_5W_{30} (1×10^{-3} mol L^{-1}, pH $\approx$ 6–7) solutions. After each adsorption step, the substrates were rinsed with water and dried under a stream of nitrogen.

Results and discussion

UV-vis spectroscopy was used to monitor the deposition process. Fig. 1 shows the UV-vis spectra of $(EuP_5W_{30}/PAH)_n$ multilayers (n = 0–6) deposited on a precursor {PEI/PSS/PAH} film on a quartz substrate. The absorption band at 225 nm in the UV-vis spectrum of the precursor (PEI/PSS/PAH) film arises from the aromatic group present in the PSS polyanion. The UV-vis spectrum of an aqueous EuP_5W_{30} solution shows three absorption bands at 211, 267 and 302 nm, so we utilized these absorption bands to monitor film growth. For the UV-vis spectrum of the multilayer films, the adsorption maxima at 267 or 302 nm cannot be observed clearly. However, plotting the absorbances at 216, 267, and 302 nm *versus* the number of (EuP_5W_{30}/PAH) layers still results in nearly straight lines (see the inset in Fig. 1), which confirms constant incorporation of EuP_5W_{30} in the multilayer. The polycation PAH does not absorb above 200 nm, and its presence in the film does not contribute to the absorption spectra. A partial loss of EuP_5W_{30} clusters after each PAH deposition step is observed in the UV-vis spectra, but the steady increase in the absorbance demonstrates that EuP_5W_{30} anions are deposited in the multilayer films.

To identify the elemental composition of the multilayer films, XPS experiments on the $(EuP_5W_{30}/PAH)_n$ (n = 1 and 4) films were carried out. Although the XPS measurements give only a semi-quantitative elemental composition, the presence of C, O, N, S, P, Eu, and W in the film is confirmed, and the expected molar ratio of 1 : 30 for Eu to W is also approximately

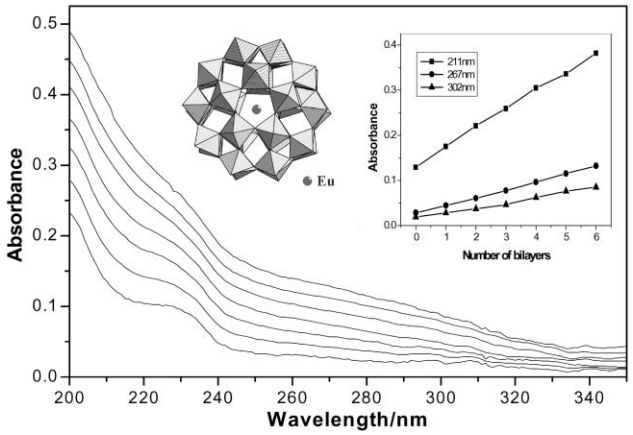

Fig. 1 UV-vis spectra of $(EuP_5W_{30}/PAH)_n$ multilayer films with n = 0–6 on PEI/PSS/PAH-modified quartz substrates (both sides). These curves, from bottom to top, correspond to n = 0,1,2,3,4,5, and 6, respectively. The inset displays both a schematic polyhedral representation of the EuP_5W_{30} cluster and the absorbance growth at 211, 267, and 302 nm as a function of the number of (EuP_5W_{30}/PAH) bilayers for the $(EuP_5W_{30}/PAH)_n$ multilayer films.

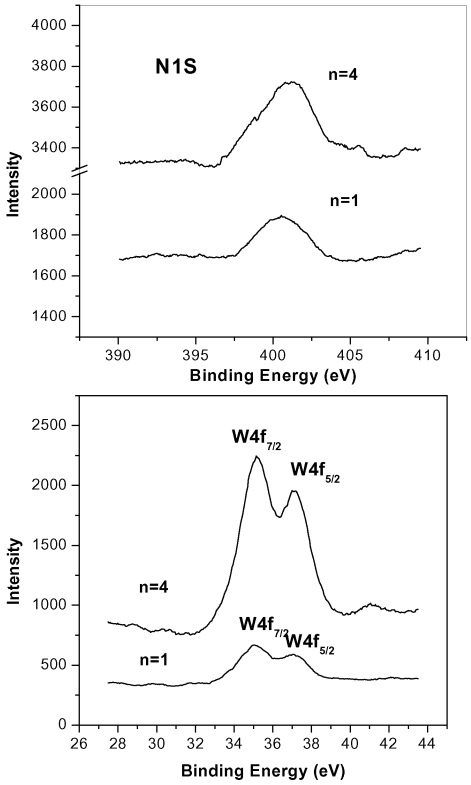

Fig. 2 X-Ray photoelectron spectra in the N(1s) and W(4f) regions for the $(EuP_5W_{30}/PAH)_n$ multilayer films with n = 1 and 4.

established. The XPS data for the $(EuP_5W_{30}/PAH)_n$ films (n = 1 and 4) are given in Fig. 2. We observed that the peak intensities of the W_{4f} and N_{1s} levels (at 35.1 and 401.2 eV, respectively) increase as the number of (EuP_5W_{30}/PAH) bilayers increases. The observed variation of the relevant peak intensities with successive depositions is clearly indicative of constant film growth as a result of LbL deposition, in agreement with the result from the UV-vis spectra. Furthermore, the presence of a single N_{1s} peak in the XPS measurements indicates that the valence state of the nitrogen atoms from PAH does not change after LbL deposition, suggesting that only a simple electrostatic interaction exists between the layers.

AFM images of the (PEI/PSS/PAH) precursor film and an additional bilayer of (EuP_5W_{30}/PAH) were taken to provide detailed information about the surface morphology and the homogeneity of the deposited films (see Fig. 3). Before EuP_5W_{30} adsorption, the outer PAH surface layer of the precursor film is uniform and smooth, with a mean roughness of 0.5 nm. After adsorption of EuP_5W_{30}, followed by adsorption of a PAH surface layer, the mean interface roughness increased to 0.848 nm. X-Ray reflectance data were collected for the multilayer films in order to investigate their structure, but no Kiessig fringes appear in the XRR curve, indicating that the film surface is inhomegeneous. In fact, a strict lamellar structure with sharp interfacial confinements between EuP_5W_{30} and PAH layers is almost impossble to reach, because the coverage of EuP_5W_{30} clusters on each layer is incomplete and inhomogenous. Without Kiessig fringes in the XRR curve, it was difficult to accurately establish the thickness of the multilayer film by this method. AFM images were therefore used to estimate the thickness of the film. The maximum peak-to-valley distance on the AFM images was considered to be approximately equal to the thickness of the {(PEI/PSS/PAH)(EuP_5W_{30}/PAH)}multilayer. The estimated thickness of the {(PEI/PSS/PAH)(EuP_5W_{30}/PAH)} multilayer film is *ca.* 6.5 nm. From previous results, it is known that under

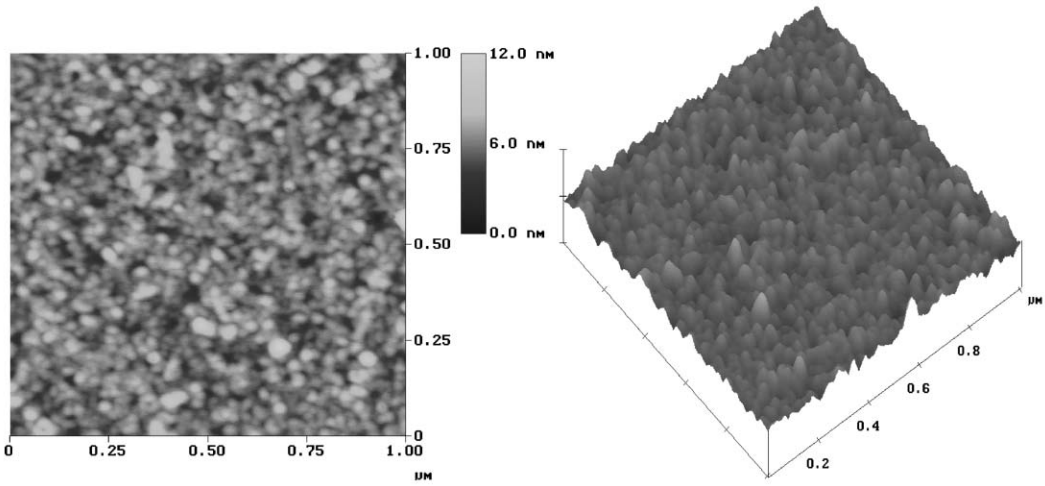

Fig. 3 Tapping mode AFM images of precursor (PEI/PSS/PAH) and [(PEI/PSS/PAH) (EuP_5W_{30}/PAH)] films.

the same experimental conditions the thickness of the precursor PEI/PSS/PAH film is 5.4 nm.[18] Based on the above-mentioned data, we infer the thickness for an {EuP_5W_{30}/PAH} layer pair to be *ca.* 1.1 nm.

Since an intramolecular energy transfer *via* oxygen-to-metal charge-transfer (O → M CT) to a lanthanide cation can occur in the polyoxometalate lattice, the photoluminescence behavior of polyoxometalates containing lanthanide cations has been investigated by various groups, including that of Yamase.[23] As shown in the inset of Fig. 1, the Eu^{3+} cation is located in the center of the $[EuP_5W_{30}O_{110}]^{12-}$ anion, which consists of a cyclic assembly of five $\{PW_6O_{22}\}$ units. The overall anion symmetry is C_{4v}, and the central Eu^{3+} cation is coordinated by a H_2O molecule that is enclosed in the central cavity.[24] For the aqueous solution of $H_n[EuP_5W_{30}O_{110}]^{(12-n)-}$ anions, the photoluminescence spectrum at 303 K displays the characteristic Eu^{3+} emission pattern consisting of $^5D_0 \rightarrow {}^7F_1$, $^5D_0 \rightarrow {}^7F_2$, $^5D_0 \rightarrow {}^7F_3$, and $^5D_0 \rightarrow {}^7F_4$ emission bands.[23] These emissions arise from the $^5D_0$ excited state of Eu^{3+} and terminate in the ^7F_J ($J = 0$–4) ground state. We determined the photoluminescence spectrum of the $(EuP_5W_{30}/PAH)_n$ ($n = 10$) multilayer film at room temperature (293 K), as shown in Fig. 4. It was well known that the $^5D_0 \rightarrow {}^7F_0$ emission band cannot be observed in the fluorescence spectra of Eu^{3+} complexes because it is forbidden according to the selection rule, unless the location of the Eu^{3+} cation deviates from the symmetry center. The $^5D_0 \rightarrow {}^7F_0$ emission band does not appear in the fluorescence spectrum of this film, as might be expected given that the Eu^{3+} cation is located in the center of the $[EuP_5W_{30}O_{110}]^{12-}$ anion. This also reflects that the $[EuP_5W_{30}O_{110}]^{12-}$ anion structure does not change after it enters the multilayer film. The fluorescence behavior of the multilayer film is essentially identical to that of the aqueous $H_n[EuP_5W_{30}O_{110}]^{(12-n)-}$ solution, except for the relative intensities and peak bandwidths. Because of the low content of EuP_5W_{30} in the multilayer film, its fluorescence intensity is weak, so the fine structure is not revealed in the multilayer film spectrum.

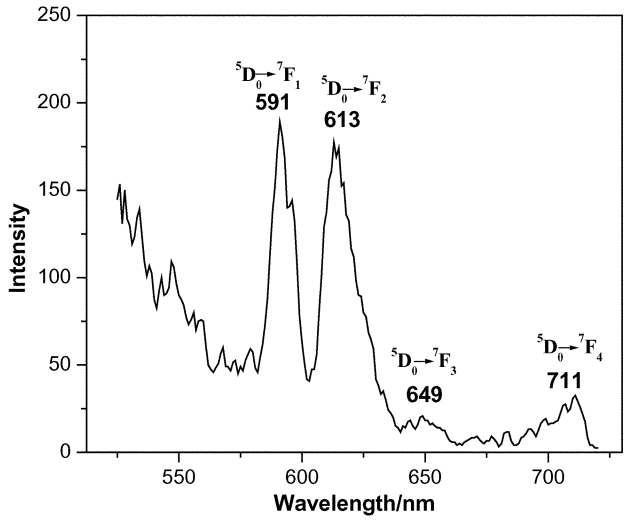

Fig. 4 Photoluminescence spectra (at 300 K) of the $(EuP_5W_{30}/PAH)_{10}$ multilayer film on quartz. The positions of $^5D_0 \rightarrow {}^7F_J$ ($J = 0$–4) emission bands are indicated in wavelength units (nm).

In consideration of the similar photoluminescent spectra of the multilayer film and the aqueous $H_n[EuP_5W_{30}O_{110}]^{(12-n)-}$ solution, it is believed that in the multilayer film the dominant interaction between EuP_5W_{30} and PAH is indeed an electrostatic attraction, so that the original coordination of Eu^{3+} is not affected. The occurence of photoluminescent activity confirms the potential for creating luminescent multilayer films with polyoxometalates and their use as functional components may be achieved by adjusting the thickness, composition, and structure of the multilayer film.

Conclusions

In this work, it has been shown that highly ordered EuP_5W_{30}/PAH multilayers can be successfully fabricated on solid substrates using consecutive layer-by-layer electrostatic adsorption. The ultrathin multilayer film has been characterized by UV-vis spectroscopy, small-angle X-ray reflectivity measurements, X-ray photoelectron spectroscopy, and AFM imaging. These reveal both regular film growth with each EuP_5W_{30} adsorption and the film thickness at nanoscale (*ca.*6.5 nm). The occurence of photoluminescent activity confirms the potential for creating luminescent multilayer films with polyoxometalates.[23]

Acknowledgement

This project was financially supported by the National Natural Science Foundation of China (grant no. 29971006).

References

1 A. Ulman, *Introduction to Thin Films: From Langmuir-Blodgett to Self-Assembly*, Academic Press, Boston, 1991.
2 G. Decher, *Science*, 1997, **277**, 1232.
3 J. Schmitt, G. Decher, W. J. Dressick, S. L. Brandow, R. E. Geer, R. Shashidhar and J. M. Calvert, *Adv. Mater.*, 1997, **9**, 61.

4 A. K. Dutta, T. Ho, L. Zhang and P. Stroeve, *Chem. Mater.*, 2000, **12**, 1042.
5 S. L. Clark, E. S. Handy, M. F. Rubner and P. H. Hammond, *Adv. Mater.*, 1999, **11**, 103.
6 X. Zhang and J. C. Shen, *Adv. Mater.*, 1999, **11**, 1139.
7 J. A. He, R. Valluzzu, K. Yang, T. Dolukhanyan, C. M. Sung, J. Kumar, S. K. Tripathy, L. A. Samuelson, L. Balogh and D. A. Tomalia, *Chem. Mater.*, 1999, **11**, 3268.
8 I. Pastoriza-Santos, D. S. Koktysh, A. A. Mamedov, M. Giersig, N. A. Kotov and L. M. Liz-Marzan, *Langmuir*, 2000, **16**, 2731.
9 M. Schütte, D. G. Kurth, M. R. Linford, H. Cölfen and H. Möhwald, *Angew. Chem., Int. Ed.*, 1998, **37**, 2891.
10 M. T. Pope and A. Müller, *Polyoxometalates: From Platonic Solid to Anti-Retroviral Activity*; Kluwer, Dordrecht, 1994.
11 C. L. Hill, *Chem. Rev.*, 1998, **98**, 1.
12 C. Hu, Y. Zhang and L. Xu, *Appl. Catal., A*, 1999, **177**, 237.
13 E. Coronado, J. R. Galan-Mascaros, C. Gimenez-Saiz and C. J. Gomez-Garcia, *Adv. Mater.*, 1993, **4**, 283.
14 N. Casan-Pastor and L. C. W. Baker, *J. Am. Chem. Soc.*, 1992, **114**, 10384.
15 T. Yamase, *Mol. Eng.*, 1993, **3**, 241.
16 D. G. Kurth, P. Lehmann, D. Volkmer, A. Müller and D. Schwahn, *J. Chem. Soc., Dalton Trans.*, 2000, 3989.
17 I. Ichinose, H. Tagawa, H. Mizuki, Y. Lvov and T. Kunitake, *Langmuir*, 1998, **14**, 3462.
18 F. Caruso, D. G. Kurth, D. Volkmer, M. J. Koop and A. Müller, *Langmuir*, 1998, **14**, 187.
19 D. G. Kurth, D. Volkmer, M. Ruttorf, B. Richter and A. Müller, *Chem. Mater.*, 2000, **12**, 2829.
20 E. Coronado and C. Mingotand, *Adv. Mater.*, 1999, **11**, 869.
21 M. Clemente-Leon, B. Agricole, C. Mingotand, C. J. Gomez-Garcia, E. Coronado and P. Delhaes, *Angew. Chem., Int. Ed. Engl.*, 1997, **36**, 1114.
22 I. Creaser, M. C. Heckel, R. J. Neitz and M. T. Pope, *Inorg. Chem.*, 1993, **32**, 1573.
23 T. Yamase, *Chem. Rev.*, 1998, **98**, 307.
24 M. H. Dickman, G. J. Gama, K. C. Kim and M. T. Pope, *J. Cluster Sci.*, 1996, **7**, 567.